



Evaluation of Supercell Storm Triggering Factors Based on a Cloud Resolving Model Simulation

Vlado Spiridonov¹ · Mladjen Ćurić²

Received: 16 March 2018 / Revised: 20 September 2018 / Accepted: 2 October 2018
© The Author(s) 2019

Abstract

An attempt has been made in this study to examine the conditional instability parameters in the selected area and to determine the main ingredients responsible for initiation and evolution of supercell storm over Skopje, Macedonia on 6 August 2016. WRF model forecasts provide the basic meteorological parameters for cloud model initialization and the detail information about atmospheric instability potential as triggering factor for severe convection. The cloud model simulation has been performed with very fine spatial and temporal resolution capable to resolve the detail aspects of convection. The results utilizing this novel method suggest that, upper level lifting, moisture advection, large CAPE, near surface convergence and increased potential vortices in the selected area play substantial role in early assessment of the atmospheric status, convective instability and storm potential. In addition the directional wind shear (veering) at the near surface layer, high storm helicity index, differential heating induced by the strong local forcing environment serve as triggering factors for initiation of supercell storm with rotational updrafts-mesocyclone. The cloud model simulation with fine resolution allows more detail insight into the storm dynamics and the mechanism of generation of rotational updrafts and mesocyclone, a hook echo signature and the presence of bounded weak echo region as ingredients for supercellular structure and evolution. The overshooting top of 15 km, peak updraft speed of 40 m/s, wind gust of 35 m/s and reflectivity which exceeds 70 dBZ indicates to the occurrence of a very severe storm. A longer live cycle of storm and the intense water production, with extreme rainfall rate of 38 mm/5 min, contribute to formation of excessive torrential rainfall and local catastrophic flooding.

Keywords Severe convection · Cloud model · Supercell storm · Flash-flooding · Ingredients

1 Introduction

Supercell storms represent the most complex and violent type of all storms. They are usually associated with producing a local excessive precipitation and flash-floods, gusty winds, large hail and even tornado (e.g. Browning 1962, 1964). The main triggering factors for their occurrence are the presence of substantial wind shear-low-level veering, large CAPE and LI

(Doswell III et al. 1996). In addition to these, the storm helicity in the layer between 0 and 3000 m, differential heating and the local forcing environment are also important factors for initiation of severe convection and supercells. Among different supercell storm types the HP supercell are responsible for heavy rainfall which are characterized by formation of quasi-steady deep rotating updrafts-mesocyclone, longer life cycle and severity. Important aspect is evolution of storms and some important processes as splitting or merging, which lead to convection intensification and occurrence of heavy rainfall and hailfall (e.g. Ćurić et al. 2009; Spiridonov et al. 2010; Ćurić and Janc 2012). Thunderstorm forecast is one of the most problematic issues in numerical weather prediction as the result of their small scale spatial and temporal resolution (Warner 2011). The increased computer resources have resulted in the possibility to use a finer spatiotemporal resolution to less than 5 km, thus allowing the explicit treatment of convection ignoring its parameterization. Many studies have been focused on using high-resolution convective permitting

Responsible Editor: Ben Jong-Dao Jou.

✉ Vlado Spiridonov
vlado.spiridonov@univie.ac.at

¹ Department of Meteorology and Geophysics, Faculty of Earth Science, Geography and Astronomy, University of Vienna, 1090 Vienna, Austria

² Institute of Meteorology, University of Belgrade, Belgrade, Serbia

simulations to study the heavy precipitation processes related to severe storms (e.g. Klemp 2006; Litta and Mohanty 2008; Litta et al. 2011; Spiridonov and Ćurić 2015). Some useful results and conclusions regarding the sensitivity of idealized supercell simulations could be found in study by Potvin and Flora (2015). The evaluation of idealized cloud model setting and sensitivity tests reveal that decreasing horizontal grid resolution from 4 to 1 km showed a more reliable simulation of storm characteristics. However, the finest grid spacing runs emphasize the question about importance of using sophisticated data assimilation of high resolution spatiotemporal observations as it is suggested by Sun et al. (2010) or convective scale data assimilation with applying non-hydrostatic convection permitting COSMO model (Baldauf et al. 2011) or employing ensemble filter (e.g. Poterjoy et al. 2017; Jacques et al. 2017) is required for improved forecast at smaller domain. In some specific in nature very severe convective cases, the models even with a suitable configuration and fine horizontal grid resolution will not be sufficient to accurate forecast of storm structural and evolutionary properties and heavy rainfall. In such cases some local scale forcing environment plays a crucial role in storm initiation and its evolution.

2 The Main Motivation

The main motivation of the present research is to evaluate the main triggering factors responsible for initiation of very severe mid-latitude convective cloud on 6th August 2016 in Skopje. At the evening hours on 6th August 2016 the wider urban and rural areas of Skopje was under influence of extremely severe weather, with the catastrophic consequences associated with torrential rainfall, gust wind, strong thunderstorm, lightning and flash flooding. During this disastrous heavy rainfall event 23 people lost their lives with huge material and economy damage. The first initiation of convective clouds started at the moon hours, in the western mountain regions of Macedonia, as a result of upper low approaching the presence of cyclonic circulation. The model has orography and it is taken through two influences: the first influence is due to the different warming of the sunny (sunny) sides and the senile (the side of the mountain in the shade), i.e., the northern slopes. This contributes to the occurrence of additional rotation in the Cb cloud vortex pair. This effect is parameterized by the method developed by Ćurić and Janc (2012). The second effect is the consequence of the channeled cold air movement that emanates from the cloud base Cb and moves along the trough. This causes the forced warm air along the front head of the cold air. Forced vertical velocity is calculated by the method of Lompar et al. (2017). In south-western flow aloft, there is a transport of moist air from southern parts of Adriatic and Ionian Seas in western and north-western parts and impact on developing of unstable weather condition

across Macedonia. The specific thermal features of the atmosphere during the current day, due to intensive heating, formation of warm air trough in the Skopje valley and the topography of the terrain generated additional favorable conditions for developing of severe thunderstorms. The most intensive processes occur in the afternoon hours, when several convective cells are initiated in the convective instability line extended over north-western parts of Macedonia, which is successively transferred in organized Mesoscale Convective System (MCS) or cluster. Finally, during the evening hours the convective processes reached the most intensive phase of evolution turning into very severe supercell storm. Considering the negative consequences of this catastrophic weather phenomenon we found very important to study in more detail and to answer on some important questions about the reasons for occurrence of such disastrous case. Thus, our main motivation is to evaluate the main storm ingredients as triggering factors for initiation and evolution of supercell storm and examination of the physical processes responsible for production of heavy rainfall and flooding.

2.1 Cloud Model Overview

The cloud model is a 3-D non-hydrostatic, compressible time-dependent, model with dynamic scheme from Klemp and Wilhelmson (1978), thermodynamics proposed by Orville and Kopp (1977), and bulk microphysical parameterization scheme (see Appendix 1) according to Lin et al. (1983). It uses a single-moment scheme for the six water categories: water vapour, cloud water, cloud ice, rain, snow and graupel or hail. Cloud water and cloud ice are assumed to be monodisperse, with zero terminal velocities. Rain, hail and snow have the Marshall-Palmer type size distributions with fixed intercept parameters. The source reference for the scheme to allow for the coexistence of cloud water and cloud ice in the temperature region of -40°C to 0°C is Hsie et al. (1980). The microphysical production terms are given in Appendix 1. The present version of the model contains ten prognostic equations: three momentum equations, the pressure and thermodynamic equations, four continuity equations for the water substances, and a subgrid-scale kinetic energy equation. More information regarding a cloud model could be found in Telenta and Aleksic (1988), and Spiridonov and Ćurić (2005), Barth et al. (2007). Boundary conditions are specified along all sides of the integration domain, since the computations take place within a finite domain. Along the top and bottom of the model domain the vertical velocity ω is set to zero. Lateral boundaries are open and time-dependent, so the disturbances can pass through with minimal reflection. Model equations are solved on a staggered Arakawa C grid (Arakawa and Lamb 1977). The horizontal and vertical advection terms are calculated by the centered fourth and second-order finite differences, respectively. Since

the model equations are compressible, a time-splitting procedure is applied in order to achieve numerical stability. With this procedure the sound wave terms are solved separately using a smaller time step, while all other processes are treated with a larger time step Δt . The scalar prognostic equations, except for pressure, are stepped from $t - \Delta t$ to $t + \Delta t$ by a single leapfrog step. The terms that are not responsible for sound wave generation in the equations of motion and pressure are calculated at the central time level t . Finally, the wind and pressure prognostic variables are stepped forward from $t - \Delta t$ to $t + \Delta t$, with forward time differencing on the small time step.

A high resolution Weather Research Forecast Non-hydrostatic Mesoscale Model WRF-NMM (see Janjic 2003) developed at the National Centers for Environmental Prediction (NCEP) has been employed to forecast this severe convective case. The model is configured to resolve a deep convection with the scale resolution, so the sub-grid cumulus parametrization is omitted. The entire grid system contains 38 layers with a terrain following hybrid sigma coordinate, and the model top is located at 50 hPa. The model uses WSM6 microphysics developed by Hong and Lim (2006), Noah Land Surface Model scheme operationally used at NCEP and Yonsei University (YSU) first order scheme Hong et al. (2006) with an explicit entrainment layer and a parabolic K-profile in an unstable mixed layer. High resolution run has been initialized using the initial and 3-hourly lateral and boundary conditions taken from NCEP GFS global longitude-latitude grid with 0.25-degree resolution, interpolated to a WRF-NMM model domain 1 shown in Fig. 1a. The cloud model is initialized under WRF conditions. The initial vertical profiles of the meteorological parameters, the potential temperature, specific moisture, u and v horizontal velocity component within (domain 2) are obtained from high-resolution WRF model forecasts. Fig. 1b shows the upper air sounding profile for Skopje case valid on 6 August 2016 1200 UTC. The forecasted upper air sounding shown on Fig. 1b, shows a low level moisture deficit due to temperature inversion, increase moisture content and strong directional wind shear in the near-surface layer. The cloud model run depends on the evaluated instability criteria and defined threshold values. A warm ellipsoid thermal bubble with minimal temperature perturbation in its centre was used to initiate convection. Through numerous cloud model simulations, emerged that averaged $0.2\text{ }^{\circ}\text{C}$ temperature perturbation is suitable for highly unstable atmosphere to trigger severe convective storm. A three-dimensional (3-D) runs were performed within small domain with size $61 \times 61 \times 20\text{ km}^3$ that covers the urban area of Skopje city. The horizontal and vertical grid resolution is 250 m, respectively. The time step of the model is 1 s and the smaller one is 0.5 s for solving the sound waves. The forecast period is 7200 s.

2.2 Method

The general principle of the method is to utilize the performances of both Weather Research Forecast WRF model and cloud resolving model in determination of the main physical processes and triggering factors responsible for development of severe convection. More specifically the proposed approach is focused on the definition of ingredients for initiation of supercell storms. It is achieved by performing a high resolution WRF forecasts with explicit treatment of convection avoiding cumulus parameterization. The hourly model outputs data are then used for both: determination of convective instability parameters and cloud model initialization. It allows a better initial meteorological input for initiation of convection with a small temperature perturbation, which is less influenced by the modeler. A three-dimensional numerical run has been performed with very fine spatiotemporal grid resolution. This suitable model configuration allows the convective processes to be resolve in more detail as key factor for understanding the structure and intensity of convective storm that could be initiated and developed under such thermodynamics and environmental conditions representative of a small volume of atmosphere. The basic supercell storm ingredients (e.g. upper low and transport of moist air, a strong low-level convergence zone, differential heating and the local strong forcing environment) for a specific domain are determined from high resolution WRF forecasts. Cloud resolving model provides an additional information about the potential for supercell storm occurrence. The rotational updrafts and downdrafts and development of meso-cyclone serve as primarily indicator for supercell initiation. The examination of microphysical parameters together with radar reflectivity fields gives more information about the life cycle of storm, its internal structure and severity, water production through various processes and assessment of the relative intensity of heavy convective rainfall.

3 Results

3.1 WRF Forecast of the Basic Ingredients for Severe Convection

Our study starts with a brief mesoscale analysis of the atmosphere and the processes which trigger mesoscale instability in Macedonia on 6 August 2016. As first in Fig. 2 we show the geopotential, temperature and wind at 500 and 850 hPa, relative humidity at 700 hPa and surface wind vectors at 10 m height. One sees approaching of upper low pressure system from west with corresponding favorable dynamical aspect of baroclinity, moist air inflow at 700 hPa and low-level convergence. A WRF-NMM 2.5 km grid forecast provides a basic physical ingredients involved in initiation of severe convection (e.g. moisture, instability, wind shear, and lifting). The

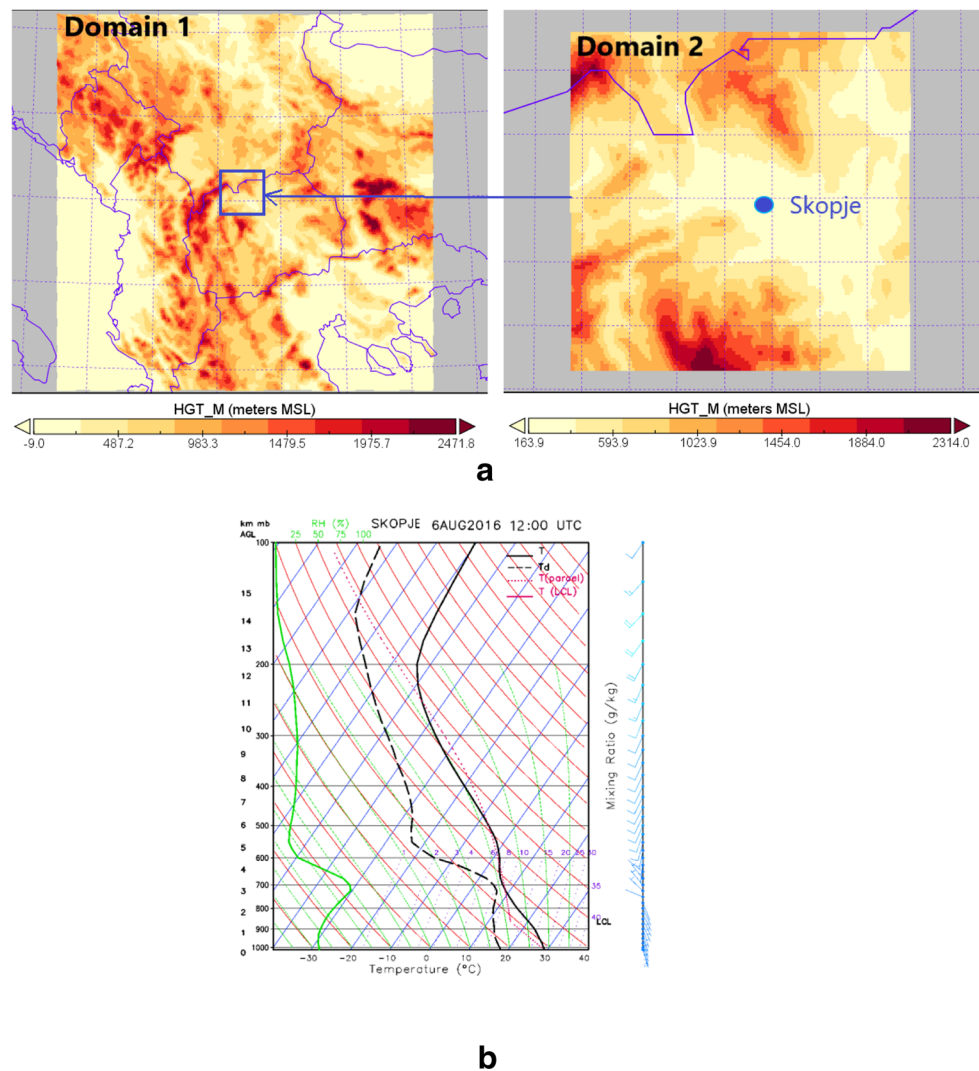


Fig. 1 a) The WRF model domain 1 and a cloud model domain 2. b) The upper air sounding profile obtained from WRF-model output in the lat/lon of Skopje, positioned in the centre of the cloud model domain

advection of warm and moist air during the day may have favored the development of thunderstorms, especially along the north-western area due to orographic lifting. The severe storms which propagated towards Skopje valley in the period between 1600 and 1800 UTC are initiated over the southwestern mountain at about the same time when the advection of moist air with high θ_e -values takes place. The fact, that storms are initiated over the complex terrain indicates that the combination of warm/moist air and orographic induced uplift played an important role. The forecast correctly captured the area with a most intense dynamics and the atmospheric disturbance. Absolute and potential vorticity displayed on Fig. 3 provide some general insights of the spin of air parcel. While there is no specific sign of distribution of absolute vorticity, potential vorticity (PV) shows some indications in respect to dynamics of convective scale weather and potential for initiation of severe storms especially in north-western portion of the model domain where positive and negative spins of the air

parcels are noted. Enhanced low-level convergence zone as result of low level moisture advection is well adjusted with the area of positive potential vorticity. As the air converges it maintains the potential vorticity, thus increases vertical updrafts leading to formation of stretched ring vortex. In addition we have also shown the distribution of atmospheric column Brunt-Vaisala frequency, which indicates that the atmosphere is statically very unstable. Other parameter important to severe thunderstorm development is wind shear. Based on the modeled results a significant vertically-sheared environment is identified over northern part which suggests that severe storms could be expected. A storm relative helicity (SRH = 300) as a measure of the amount of rotation found in storm's updraft and the potential for cyclonic updraft rotation indicates a very favorable conditions to supercell development over north-western part and urban and rural areas of Skopje valley. Another important conditionally instability parameter for the formation of a thunderstorm is the surface Convective

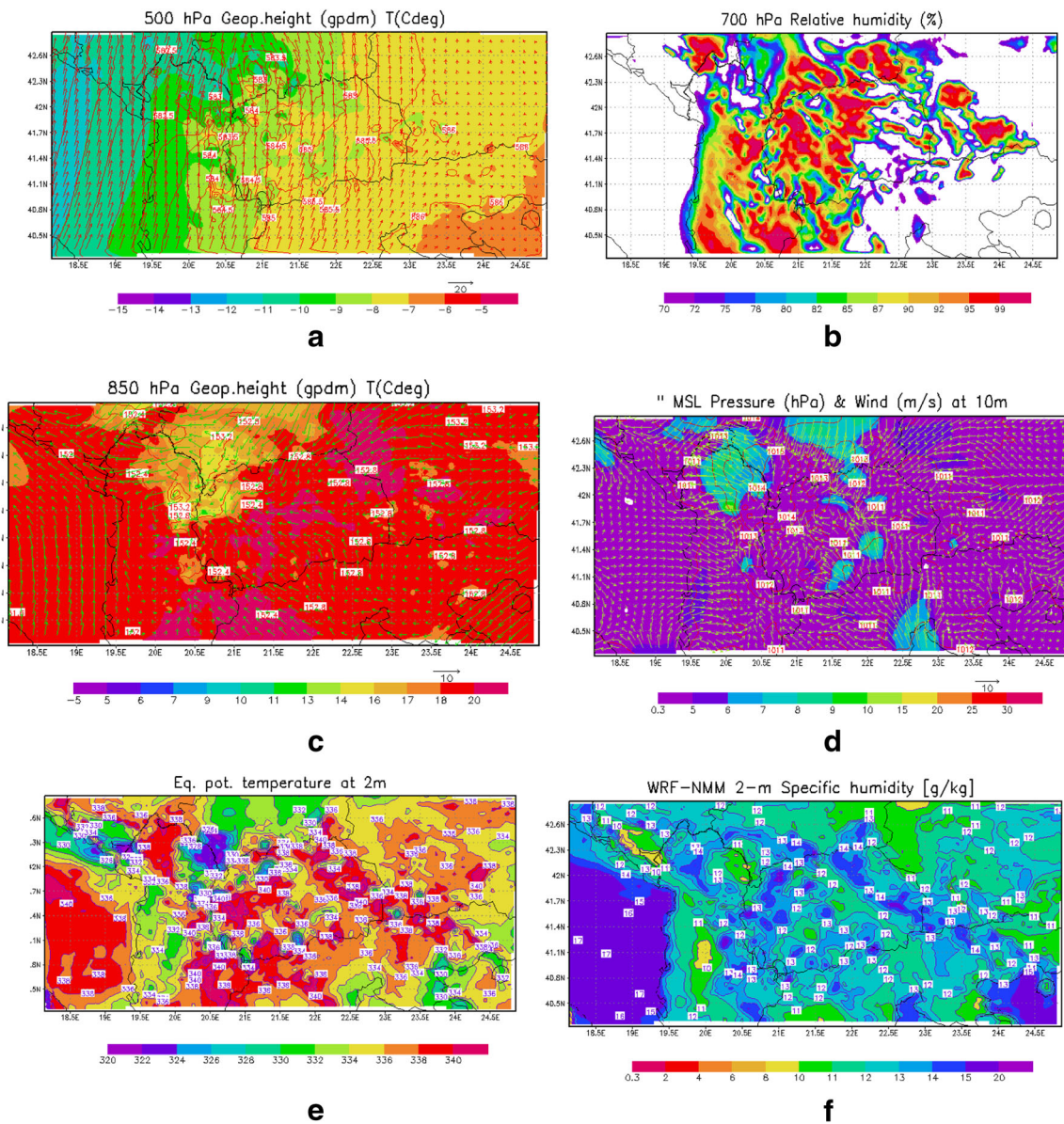


Fig. 2 a) WRF-NMM 2.5 km grid forecast for 6 August 2016 12:00 UTC: a) 500 hPa geopotential height (gpdm), temperature ($^{\circ}\text{C}$) and wind (m/s); b) RH at 700 hPa level; c) same as (a) but for 850 hPa; d)

MSL pressure (hPa), temperature ($^{\circ}\text{C}$) and wind (m/s); e) equivalent potential temperature θ_e (K); and f) specific moisture at the surface (g/kg)

Available Potential Energy (CAPE). CAPE is a measure for the amount of energy available for convection. While much of the northern part of Macedonia which is under the moderate CAPE values, south-western mainly mountain part shows a high CAPE, ranging from 2000 to 2500 and Lifted Index LI from 6 to 8, indicate that the storms will be very severe. In addition we have consider important to examine the modeled top of the brightness temperature as important ingredient of severe convection. Fig. 4 shows distribution of forecasted top brightness temperature on 6 August from 1500 to 1800 UTC. One sees a three major convective cores with temperature which is lower than 50°C . These patterns indicate areas where deep convection is developed. The modeled distributions of a

brightness temperature coincide well with satellite image in respect to location, timing and temperature rate. It is a good indicator of initiation of very severe convective clouds with overshooting tops. This quasi-stationary convective system with many convective cells reach maturity and produce extreme rainfall over Skopje valley causing flash flooding. One of the key parameter for determining the storm structure, evaluation and the intensity is the radar reflectivity. The maximum radar reflectivity fields from 15:00–18:00 UTC are displayed on Fig. 5 The convective system with a group of organized cells extend from south-western region moving towards east-northeast passing over Skopje city. Around 16:00 UTC supercell storm evolves form this system in its frontal flank with reflectivity of about 65

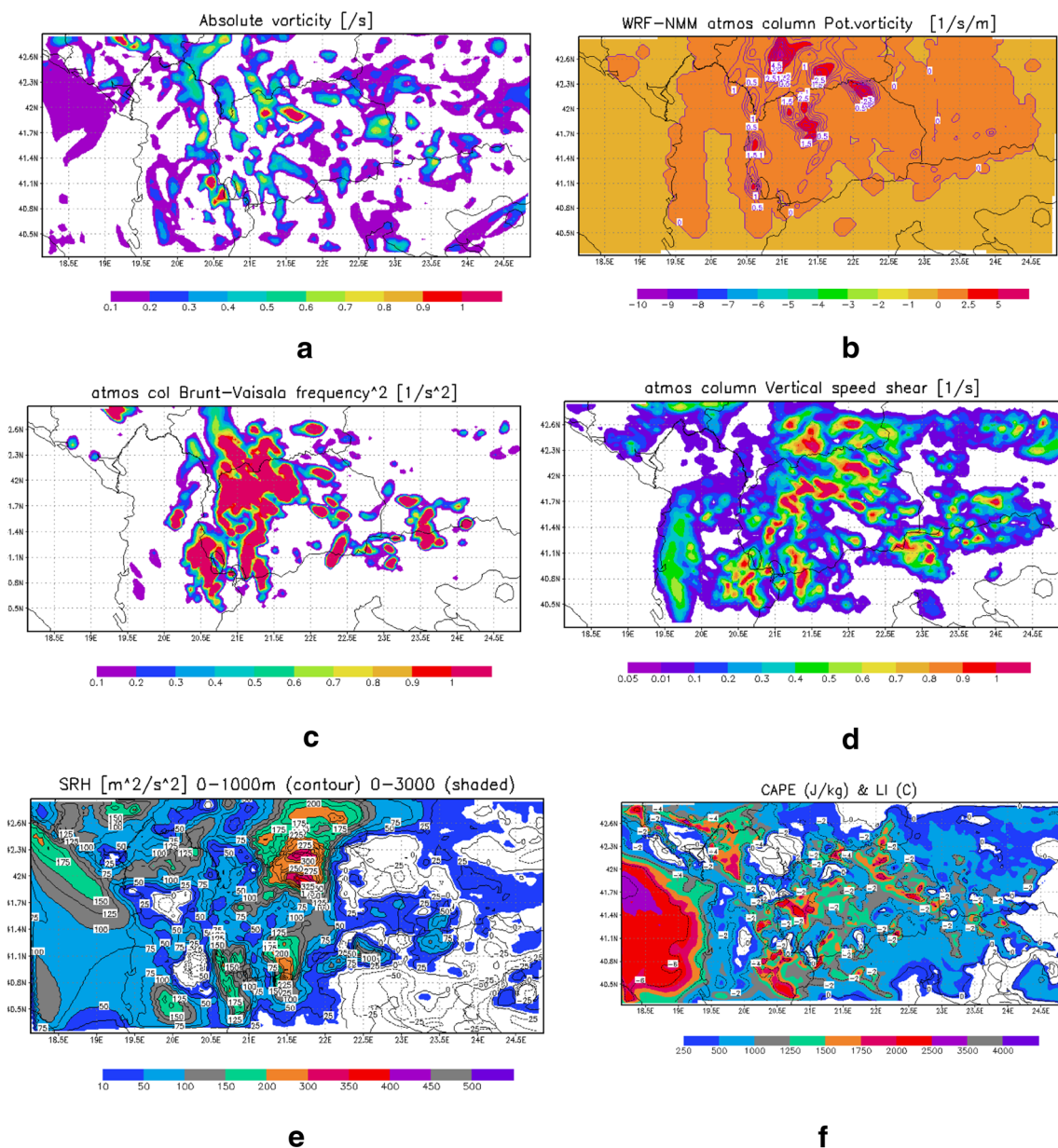


Fig. 3 WRF-NMM 2.5 km grid forecast for 6 August 2016 15:00 UTC: **a)** absolute vorticity potential vorticity (s^{-1}); **b)** atmospheric column potential vorticity (mass-weight) ($1/s/m$); **c)** atmospheric column Brunt-Vaisala frequency ($1/s^2$); **d)** atmospheric column vertical wind shear ($1/s$);

e) Storm relative helicity (m^2/s^2) 0-1000 m (contour) and (0-3000 m) shaded; **f)** Surface Convective Available Potential Energy CAPE (J/kg) and Lifted Index LI ($^{\circ}C$)

dBZ. The strongest reflectivity signature well agrees with the forecast of heavy precipitation area positioned over Skopje valley. As can be seen from Fig. 6, the period of most intense rainfall occurs from 1600 to 1700 UTC and corresponds well with the maximum radar reflectivity patterns. During that period high rainfall rates are evident with the relative intensities ranging from 25 to 30 mm/h. All these ingredients indicate appearance of heavy precipitation supercell storm with extreme rainfall over the urban area of Skopje city. As the summary, WRF-NMM forecast provides a good initial information about meso-scale atmospheric processes and instabilities as triggering factors for initiation of

severe convection. An upper level low pressure system, moisture advection and high energy were favorable factors for atmospheric destabilization and occurrence of severe convection. The distribution of moisture, instability, lift and wind fields serve as primarily factors have a profound influence on convective storm type and supercell. The existence of many other ingredients (e.g. low-level convergence, vorticity) and localized strong forcing environment induced by the topography of the terrain and the differential heating represent a key ingredients for temperature perturbation and initiation of a deep mist convection.

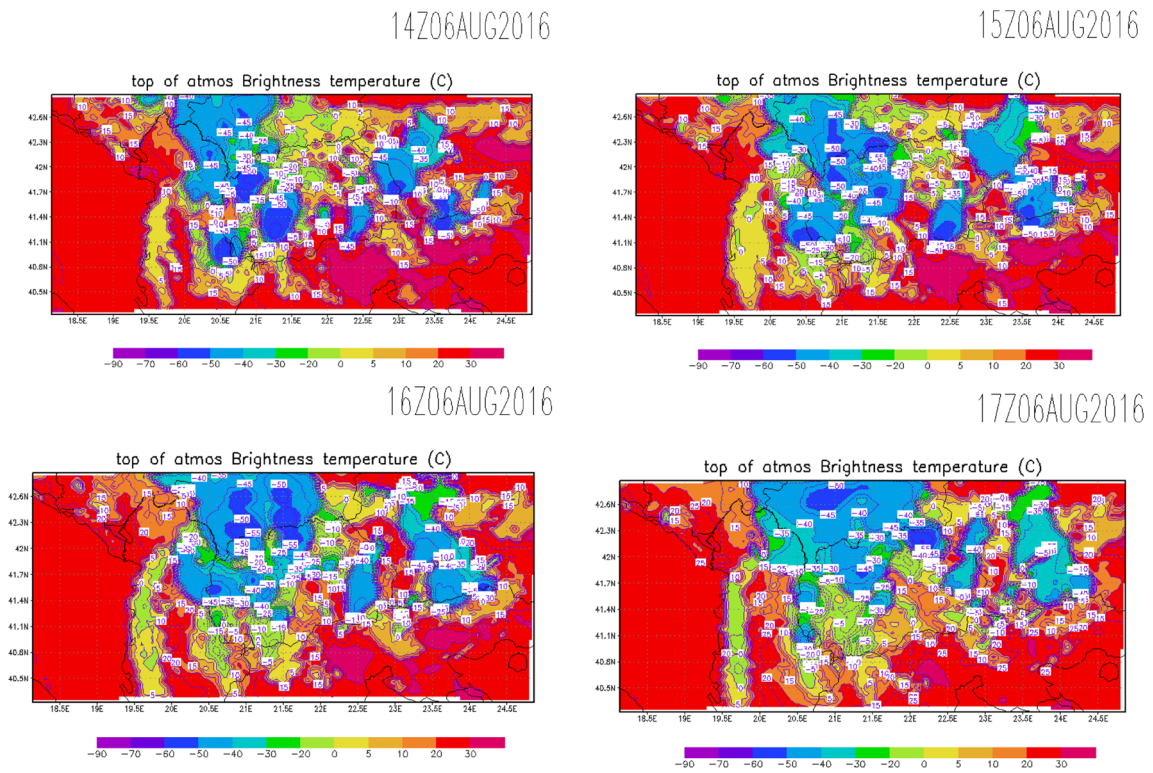


Fig. 4 WRF-NMM 2.5 km grid forecast of top of atmospheric brightness temperature (°C) for 6 August 2016 from 15:00 to 17:00 UTC

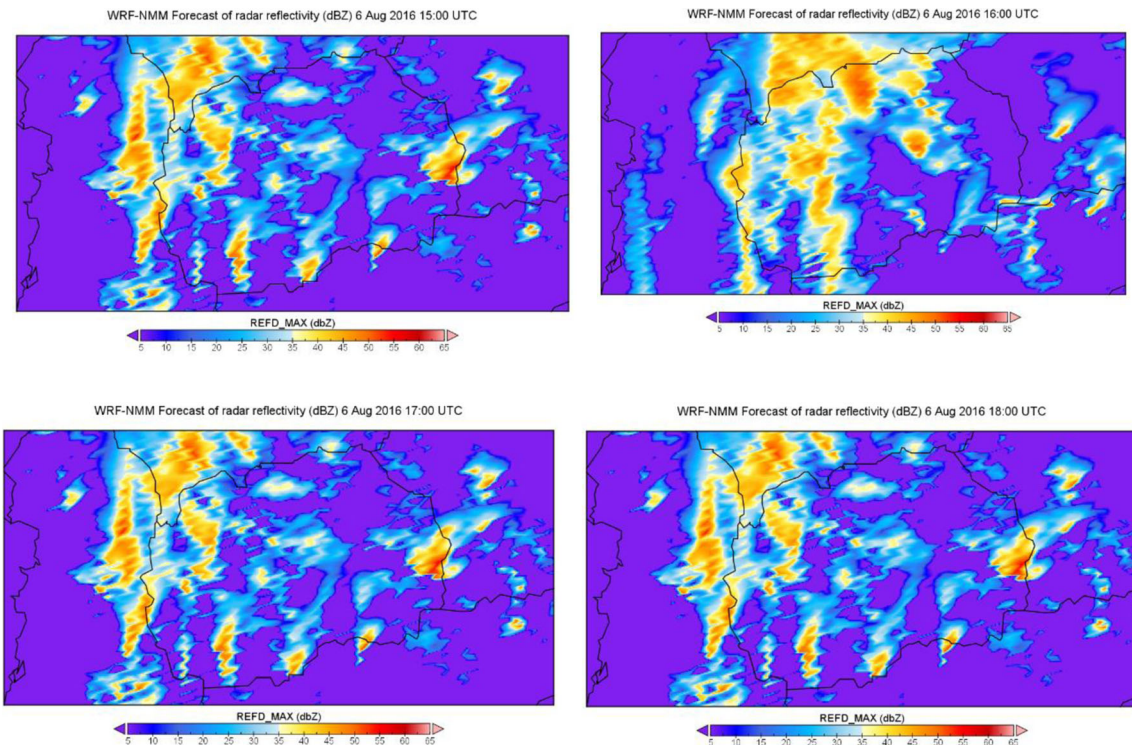


Fig. 5 WRF-NMM 2.5 km grid forecast of the maximum radar reflectivity (dBZ) for 6 August 2016 from 15:00 to 18:00 UTC

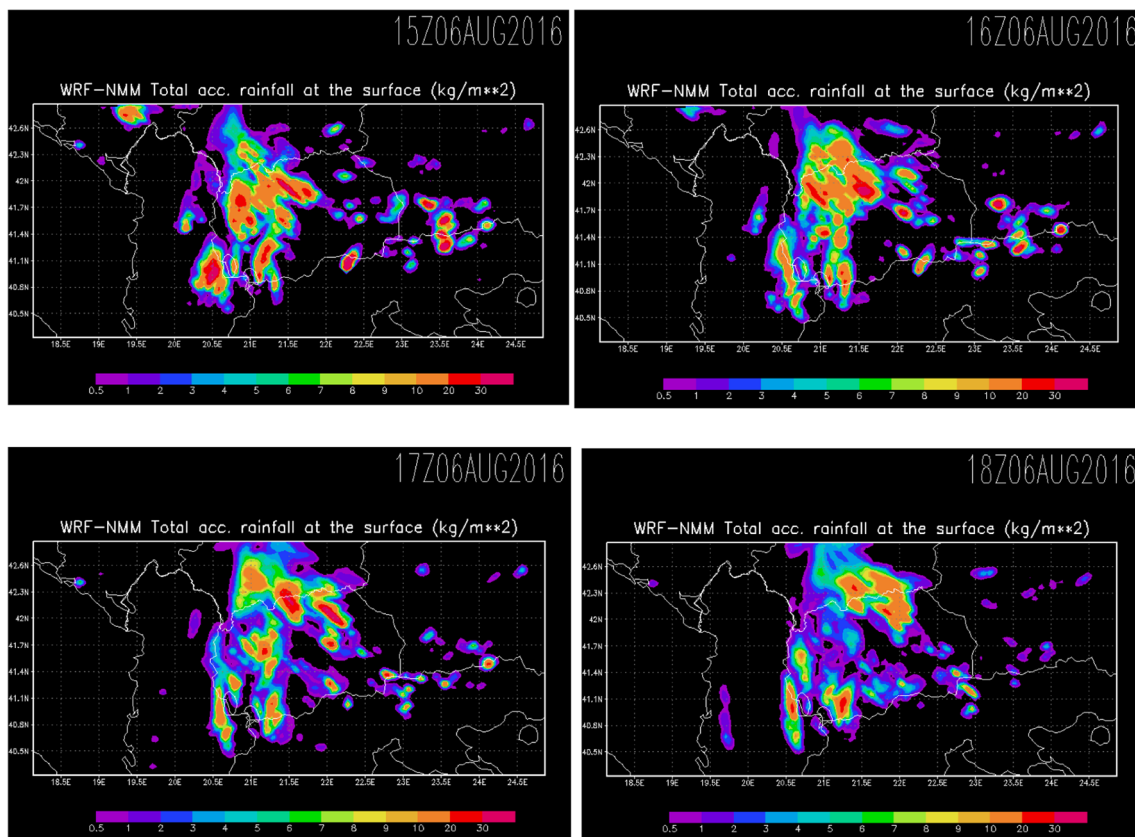


Fig. 6 WRF-NMM 2.5 km grid forecast of hourly accumulated precipitation (kg/m^2) for 6 August 2016 from 15:00 to 18:00 UTC

3.2 A Three-Dimensional Numerical Simulation

A supercell storm developed over Skopje was a long-lived (greater than 1 h) associated with a strong winds, heavy rainfall and hailfall, weak-to-strong tornado and flash flooding causing large material damages even more the human losses. All above forecasted derived parameters provide a good initial information about the thermodynamic status of atmosphere as basic triggering factors for development of severe convection. A more detail insight in the physical processes responsible for initiation of supercell storm is provided by employment of a cloud model that is initialized from WRF-NMM vertical profile data inserted in the cloud model domain. Fig. 7 shows some initial results from a three-dimensional numerical simulation, associate with a complex storm dynamics and microphysics. We present cloud sequences at the most intense phase of evolution of the storm life cycle when rotating updrafts developed with mesocyclone and existed for a few hours which was critical aspect for the flash flooding occurrence. The strong updrafts regions are usually compensated with downdrafts. For better illustration the conceptual model of mesocyclone is also shown. In respect to microphysics, the upper portion of simulated storm contains ice crystals and snow particles, while in the middle part supercooled water, graupel or hail and rainwater coexist. The sub-cloud area has a two zones with heavy rainfall. A more detail evaluation of

the storm structural and evolutionary processes is given in the next topic. A three-dimensional evolution of the storm depicted on Fig. 8 during simulation time provides a more detail insight in storm structure and severity. The light grey belts delineate the areas with cloud ice and the supercooled water content, dark grey color shows the regions with formation of graupel or hail stones, yellowish color which is viewed at the upper portion of storm in the characteristic anvil area, at the negative temperatures, marks the snow crystals, and the green areas display the heavy rainfall zones. Undoubtedly is the fact that the three-dimensional depiction of the convective cloud system over Skopje gives realistic structural picture and intensity, as well as the type of this supercell storm.

3.3 Supercell Storm Based Ingredients

Our research continues with examination of the main ingredients responsible for initiation of supercell convection and the physical processes participate in production of heavy rainfall and flooding. That is achieved by using a 3-d cloud model with fine space and temporal grid resolution which is sufficient to resolve the convective processes in more detail. The initial analyses imply on occurrence supercell storm with rotating updrafts and mesocyclone. The mesocyclone which developed over the Skopje valley represents the vorticity system, with strong rotating updrafts of air, formed into powerful

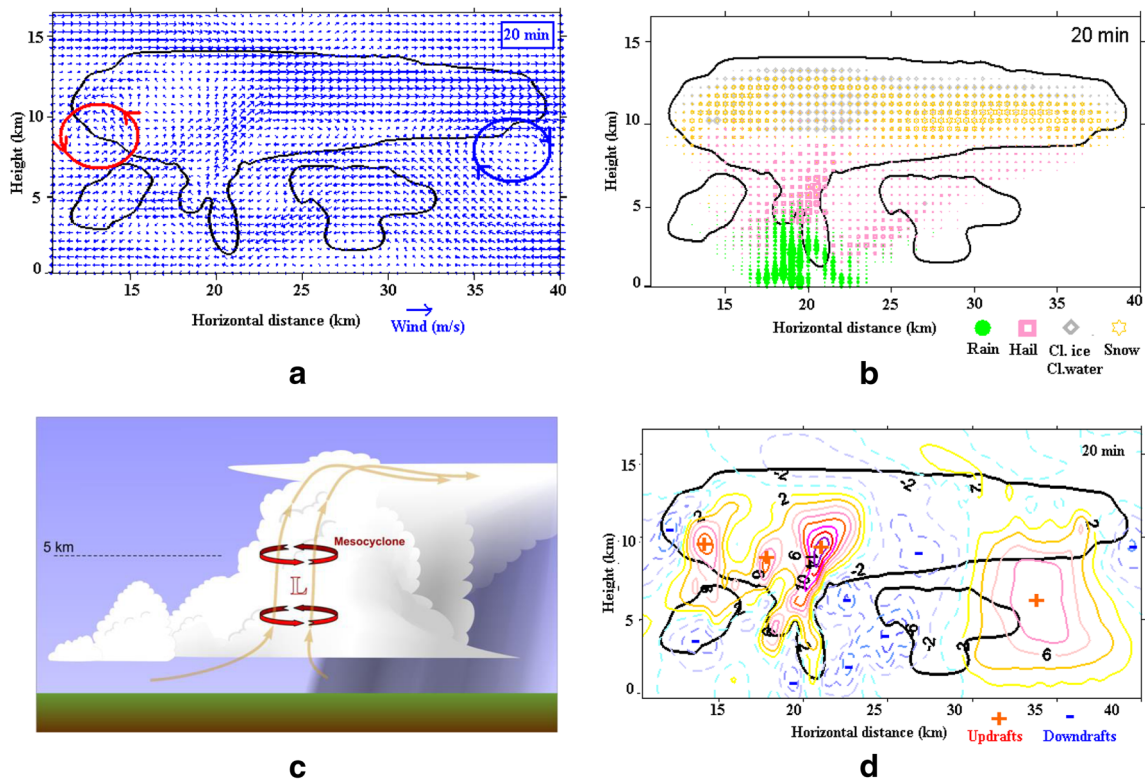


Fig. 7 a) Vertical wind vectors in convective storm on 6 August 2016; b) The microphysical structure of severe storm at 20 min of the simulation time. c) The conceptual model of mesocyclone. Source: The

supercell storm. To verify and document the significance of occurrence of mesocyclone we have calculated the vertical component of vorticity equation and all terms included in the vorticity equation in order to determine the important

Pennsylvania State University-Department of Meteorology. d) Vertical profile of updrafts and downdrafts regions within simulated storm

contributors for initiation and formation of supercell storm. Actually, we have examined the relative magnitudes of each term in the vertical component of vorticity equation in $(x, y, z,$ and $t)$ given by the following relation:

$$\frac{\partial \zeta}{\partial t} = -u \frac{\partial \zeta}{\partial x} - v \frac{\partial \zeta}{\partial y} - w \frac{\partial \zeta}{\partial z} - v \frac{\partial f}{\partial y} - (\zeta + f) \left(\frac{\partial u}{\partial x} + \frac{\partial v}{\partial y} \right) - \left(\frac{\partial w}{\partial x} \frac{\partial v}{\partial z} - \frac{\partial w}{\partial y} \frac{\partial u}{\partial z} \right) + \left(\frac{\partial F_{ry}}{\partial x} + \frac{\partial F_{rx}}{\partial y} \right) + \frac{1}{\rho^2} \left(\frac{\partial \rho}{\partial x} \frac{\partial p}{\partial y} - \frac{\partial \rho}{\partial y} \frac{\partial p}{\partial x} \right) \quad (1)$$

Here $\frac{\partial \zeta}{\partial t}$ denotes the rate of change of the relative vorticity at a grid point. The other terms on the r.h.s. of the Eq. (1) represent: the zonal advection, meridional, vertical transfer of relative vorticity, advection of planetary vorticity, divergence term, tilting or twisting, friction and solenoidal term, respectively. Fig. 9 shows relative vorticity distribution at different heights. Note that blue curves delineate increase rate of change of relative vorticity and red curves indicate decrease rate of change of relative vorticity. At the surface there is a narrow region with positive vorticity as the result of relatively high convergence at the near surface layer. There are also a few isolated divergence zones which contribute to decrease vorticity. A dramatic increase in vorticity at all levels is evidenced, mainly as the result of the PVA (zonal advection) at 1.5 km height and convergence, meridional advection and vertical transfer of relative vorticity at 3.0 km. (see Fig. 10).

There is also contribution coming from the rate of change of the vertical velocity in the horizontal direction which impairs a tilting and spinning effect, although the rates are much lower compared to the other terms. The distribution of relative vorticity at 3.0 km height during simulation time is depicted on Fig. 11. It is obvious that individual pair of vortices with positive and negative signs is seen at the initial phase of storm evolution from 5 to 10 min of the simulation time. A significant increase in relative vorticity is simulated once storm enters its intense phase of evolution, especially in 30 min, when two cores with higher vorticity gradient are determined.

The research continues with evaluation of the relative importance of the vorticity terms during simulation time (see Fig. 12). One sees that in the initial phase relative vorticity is gradually increased due to horizontal advection which turns horizontal vorticity into the vertical component through

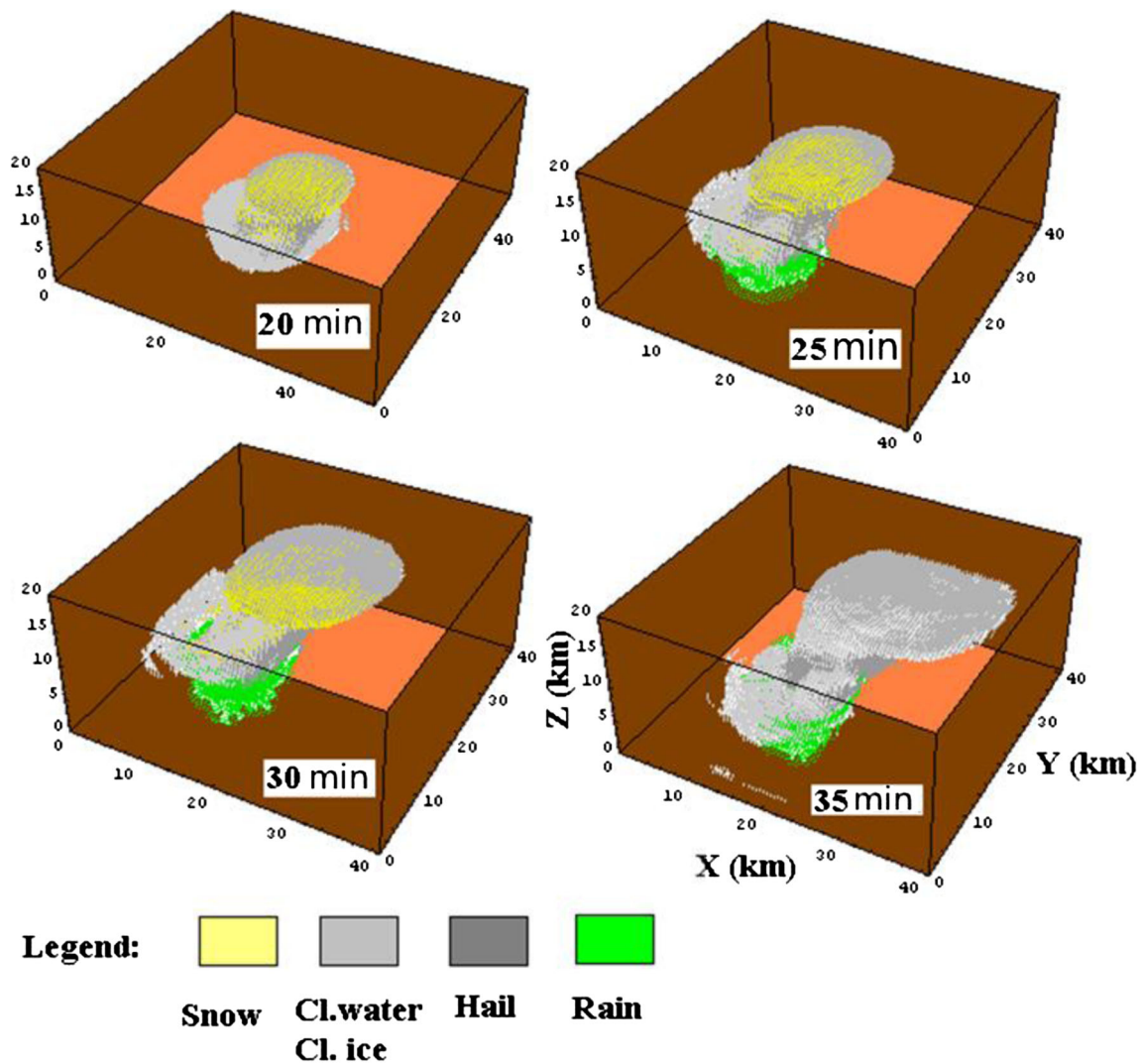


Fig. 8 A three-dimensional view of supercell storm over Skopje on 6 August 2016 viewed from SW-NE during most intense stage of evolution

differential vertical motion. How storm is moving from its incipient to mature phase divergence term and the vertical transfer play a significant role in the magnitude of relative vorticity. Around 17:25 (25 min simulation time) a dramatic increase is evidenced when it reaches a peak value of -2.942 s^{-2} . The second maximum is calculated 20 min later but this time divergence, zonal and meridional advection and the vertical transfer term, have a similar contribution rates to high relative vorticity.

Based on radar observation and the modeling studies of fluid motion it is found that in general the intense vertical vortices in the cloud originate from a vortex with a horizontal axis. This usually occurs in the storm development phase when the horizontal component of the vorticity tilts, intensifies and transforms into a vertical vorticity. The development of midlevel rotation updrafts and mesocyclone can also be demonstrated by using the vertical vorticity component written as

$$\frac{d}{dt}(\zeta + f) = (f + \zeta)w_z + (\xi w_y + \eta w_x) \tag{2}$$

Ignoring the Coriolis parameter, and linearize this equation under condition.

$\vec{v} = (\bar{u}, 0, 0)$, we obtain the equation of vorticity perturbation

$$\zeta'_t + \bar{u}\zeta'_x = \bar{u}_z w_y \tag{3}$$

If one sees the situation that the storm is moving at a speed \bar{u} , then in a system that moves with the cloud, it is obtained from (3) that

$$\zeta'_t \approx \bar{u}_z w_y \tag{4}$$

It can be seen that perturbed vorticity ζ' happens as a result of a twisting term of vortex tube. The updrafts with positive and negative vorticity perturbation ζ' , respectively are

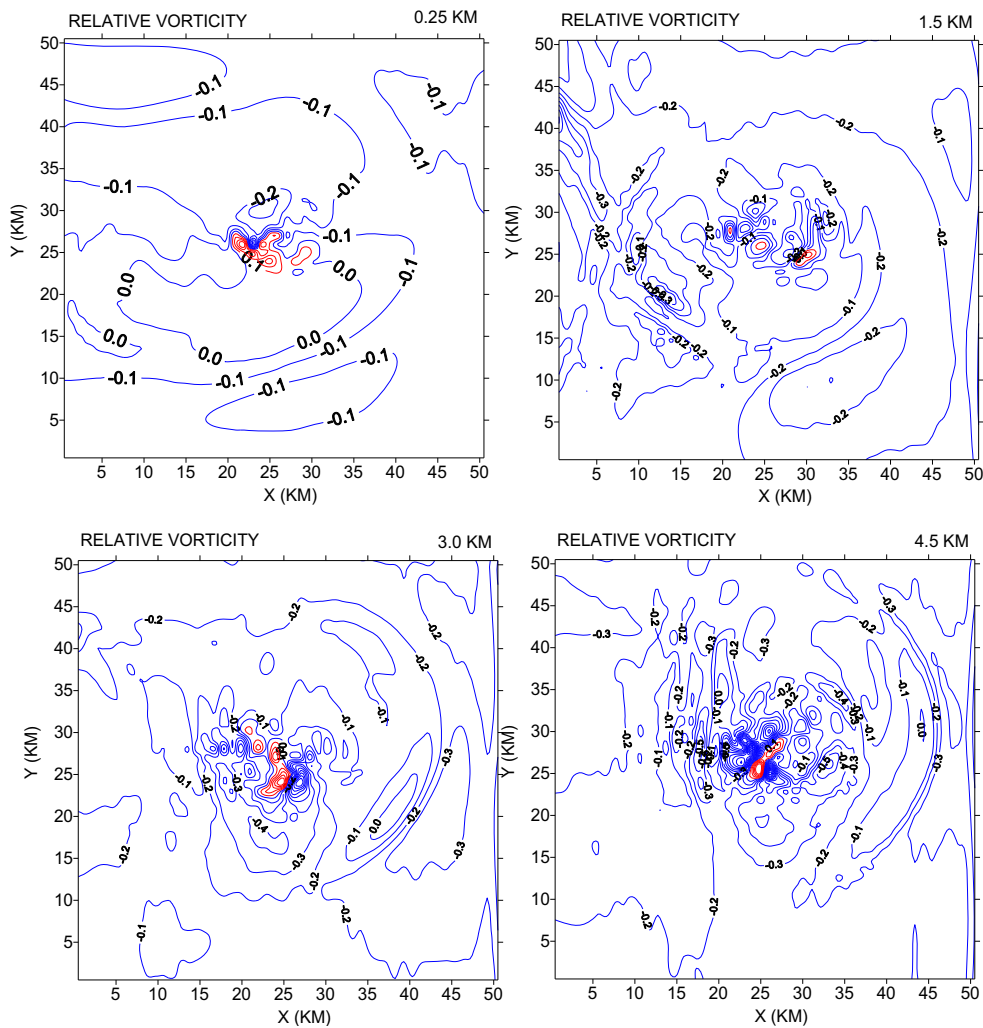


Fig. 9 Horizontal cross-sections of the simulated vertical vorticity at 0.25, 1.5, 3 and 4.5 km height in 25 min of the simulation time during the most intense phase of storm evolution on 6 Aug 2016, 1600 UTC

generated on l.h.s. and r.h.s of cloud as it is shown in Fig. 7. The direction of rotation of vortex pair serves as triggering factor of the entrainment processes within cloud. When the cloud with a pair of vortices develops further, then non-linear effects became more evident. They would be seen in a linearized equation (4), in which a nonlinear term $\zeta'w_z$ would also be retained. Then the equation for disturbed vertical vorticity component is given, also in the following form:

$$\zeta'_t + \bar{u}\zeta'_x \approx \bar{u}_z w_y + \zeta'w_z \tag{5}$$

Areas with high values of (w_z) are located at the top and bottom of the updrafts region. The “stretching” term ($\zeta'w_z$) is also important as a twisting term. After storm splitting, a two new generated clouds move along y-axis away from each other. The storm movement could be considered relative to the ground with velocity

$$\vec{v}_c = u_c \vec{i} + v_c \vec{j} \tag{6}$$

At the non-divergent level of cloud $\bar{u} \approx u_c$. Then the vorticity perturbation equation is

$$\zeta'_t - v_c \zeta'_y \approx \bar{u}_z w_y \tag{7}$$

Hence, in stationary case we get

$$\zeta' \approx \frac{\bar{u}_z}{v_c} w \tag{8}$$

It is evident that the maximum vorticity disturbance ζ' occurs in the area of maximum vertical velocity (w). The splitting part of the storm with right movement has a positive vorticity $\bar{u}_z > 0$. On this way a rotating updraft could be developed at the middle levels of an intense C_b clouds. Such rotating updraft referred as mesocyclone represents the largest and most important part of storm where tornado genesis is a common case. The mesocyclone basically represents one the most severe atmospheric weather phenomena of all types of storms.

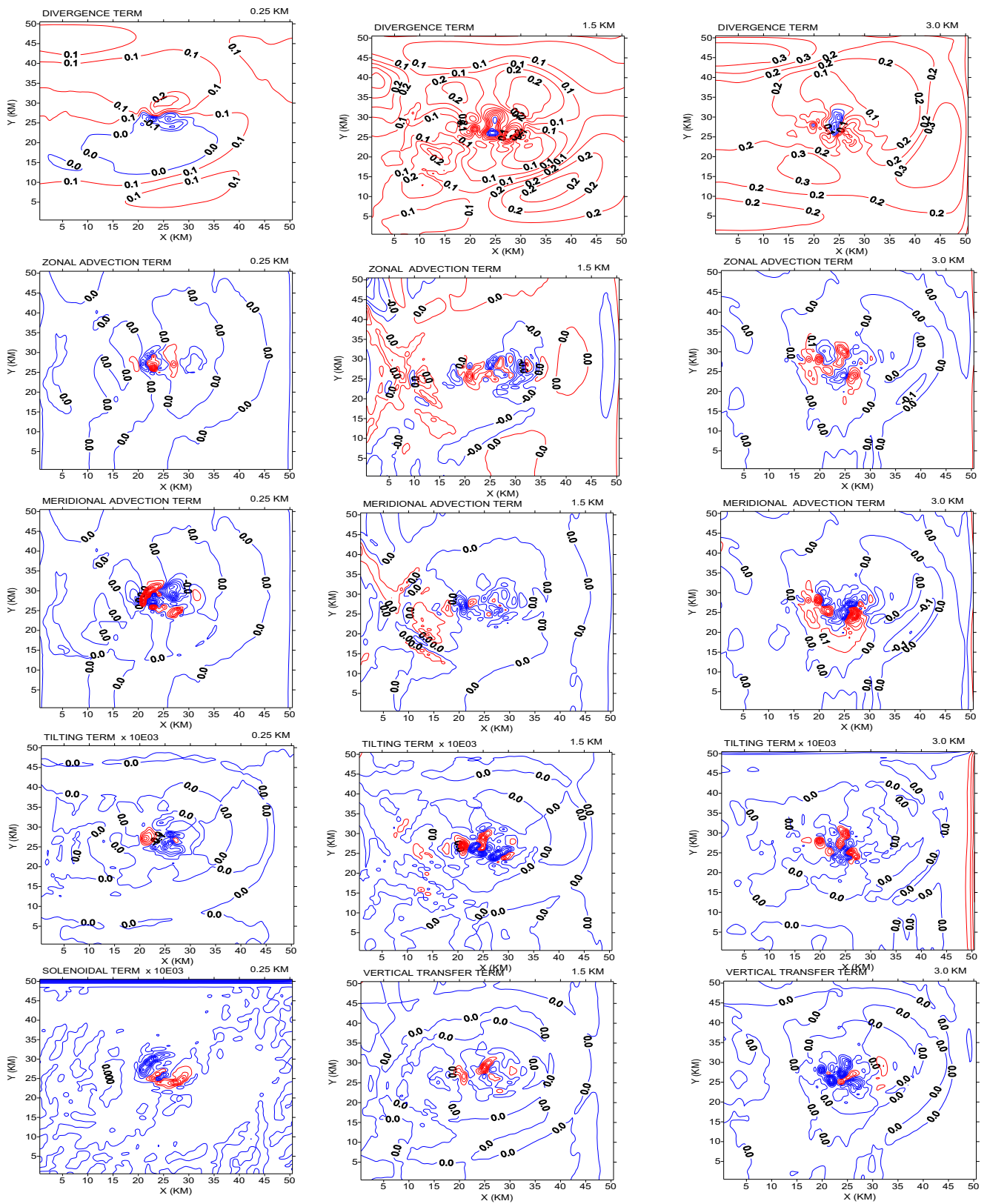


Fig. 10 Horizontal distributions of various terms of relative vorticity at 0.25, 1.5 and 3.0 km height at the most intense phase of storm evolution

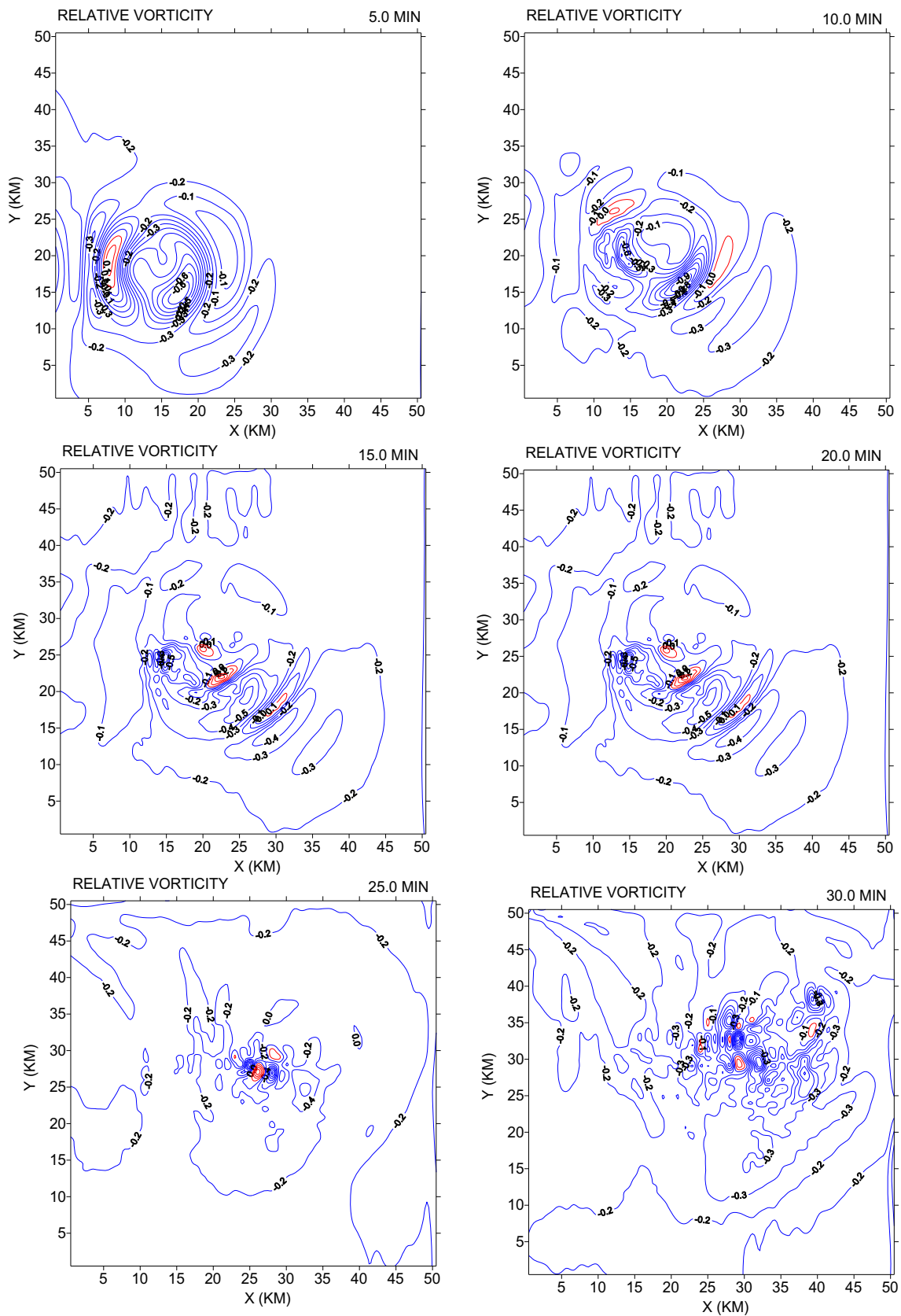


Fig. 11 Horizontal cross sections of the relative vorticity (s^{-2}) at 3 km height from 5 to 40 min of the simulation time at each 5 min intervals

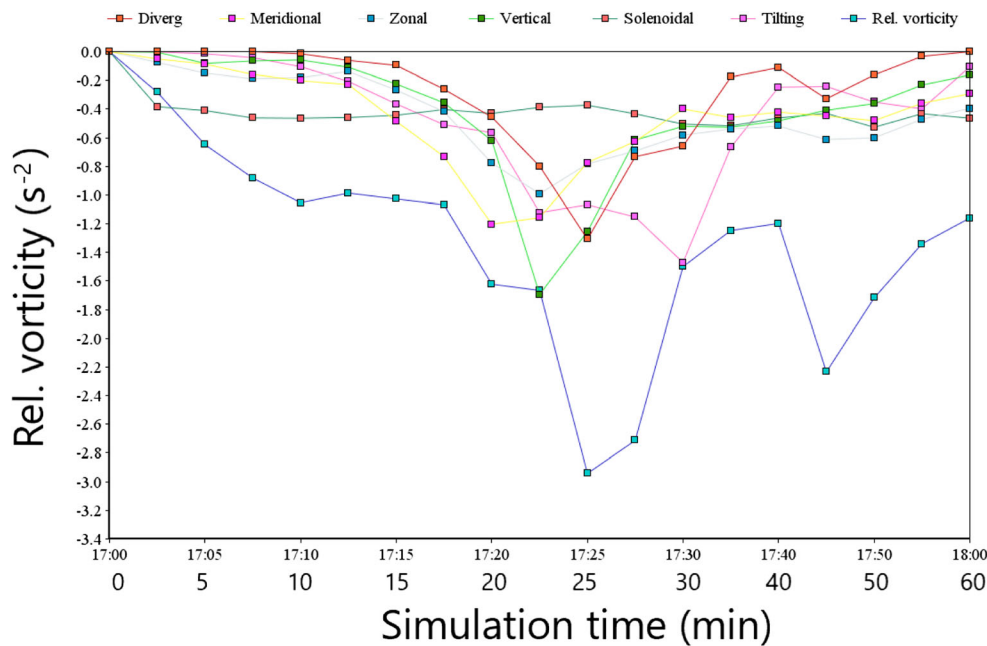


Fig. 12 Time evolution of divergence, meridional, zonal, vertical transfer, solenoidal and tilting (twisting) term which contribute in increase of rate of change of relative vorticity (s^{-2}) at grid point during simulation time

Our study follows with examination of the microphysical processes responsible for storm intensity and production of large amount of rain Table 1 list the microphysical production terms for water vapor, cloud water, cloud ice, rainwater, snow and hail averaged over simulation time. The main contribution to increase cloud water content comes from the accretion process of cloud water by graupel, (PGACW) with production rate of about 1.0×10^{-4} ($kg\ kg^{-1}\ s^{-1}$). All other production terms have lower contribution rates. In respect to cloud ice the key microphysical process based on the model calculations is the accretion of cloud ice by graupel (PGACIP) with 10 times lower rate relative to (PGACW). Regarding the snow production the dominant one is the production rate for accretion of snow by graupel (PGACSP). It is evident that

production rate for accretion of rain by cloud ice, snow and hail (PIACR, PSACR and PGACR) appear to be the most important processes regarding the large production of rain in the simulated storm with averaged rates (3.24×10^{-4} , 1.10×10^{-4} and 1.57×10^{-4}) respectively. In addition to all these microphysical transfer rates the responsible process to formation of rain is graupel melting to form rain at $T \geq T_0$ (PGMLT). The simulation of radar reflectivity field evolution whose maximum value exceeded 70 dBZ, tells us much more about the storm structure and intensity and detection of region with limited radar echo aloft, which occurs when strong updrafts of storm suspend and suspect the rainfall to be formed and fallout. The location of this radar echo coincides with the center of mesocyclone (rotating updraft) as it is illustrated in the Fig. 7c, d.

Table 1 The mean transfer rates ($kg\ kg^{-1}\ s^{-1}$) of the microphysical processes averaged over 2 h simulation period

Water vapor-QRR ($kg\ kg^{-1}\ s^{-1}$)	Cloud water-QLCW ($kg\ kg^{-1}\ s^{-1}$)	Cloud ice-QLCI ($kg\ kg^{-1}\ s^{-1}$)	Rainwater-RA1 ($kg\ kg^{-1}\ s^{-1}$)	Snow SN1 ($kg\ kg^{-1}\ s^{-1}$)	Hail HA1 ($kg\ kg^{-1}\ s^{-1}$)
PSDEP 7.76×10^{-7}	PRAUT 2.82×10^{-6}	PSAUT 1.24×10^{-6}	PREVP -1.64×10^{-5}	PSMLT -1.85×10^{-6}	PGMLT -9.33×10^{-5}
	PRACW 3.77×10^{-13}	PSACI 1.17×10^{-5}	PIACR 3.24×10^{-4}	PGAUT 2.03×10^{-7}	PGSUB -9.72×10^{-7}
	PSACW 2.41×10^{-5}	PRACI 2.02×10^{-14}	PSACR 1.10×10^{-4}	PRACS 2.78×10^{-5}	
	PGACW 9.59×10^{-5}	PSFI 1.27×10^{-5}	PGFR 9.70×10^{-6}	PSSUB -1.91×10^{-6}	
	PSFW 1.36×10^{-8}	PGACI 1.82×10^{-6}	PGACR 1.57×10^{-4}	PGACS 1.19×10^{-5}	
		PGACIP 1.82×10^{-5}	PGACRP 2.52×10^{-5}	PGACSP 4.96×10^{-5}	

Terms with bold letters indicate the most dominant cloud physics processes during model simulation time

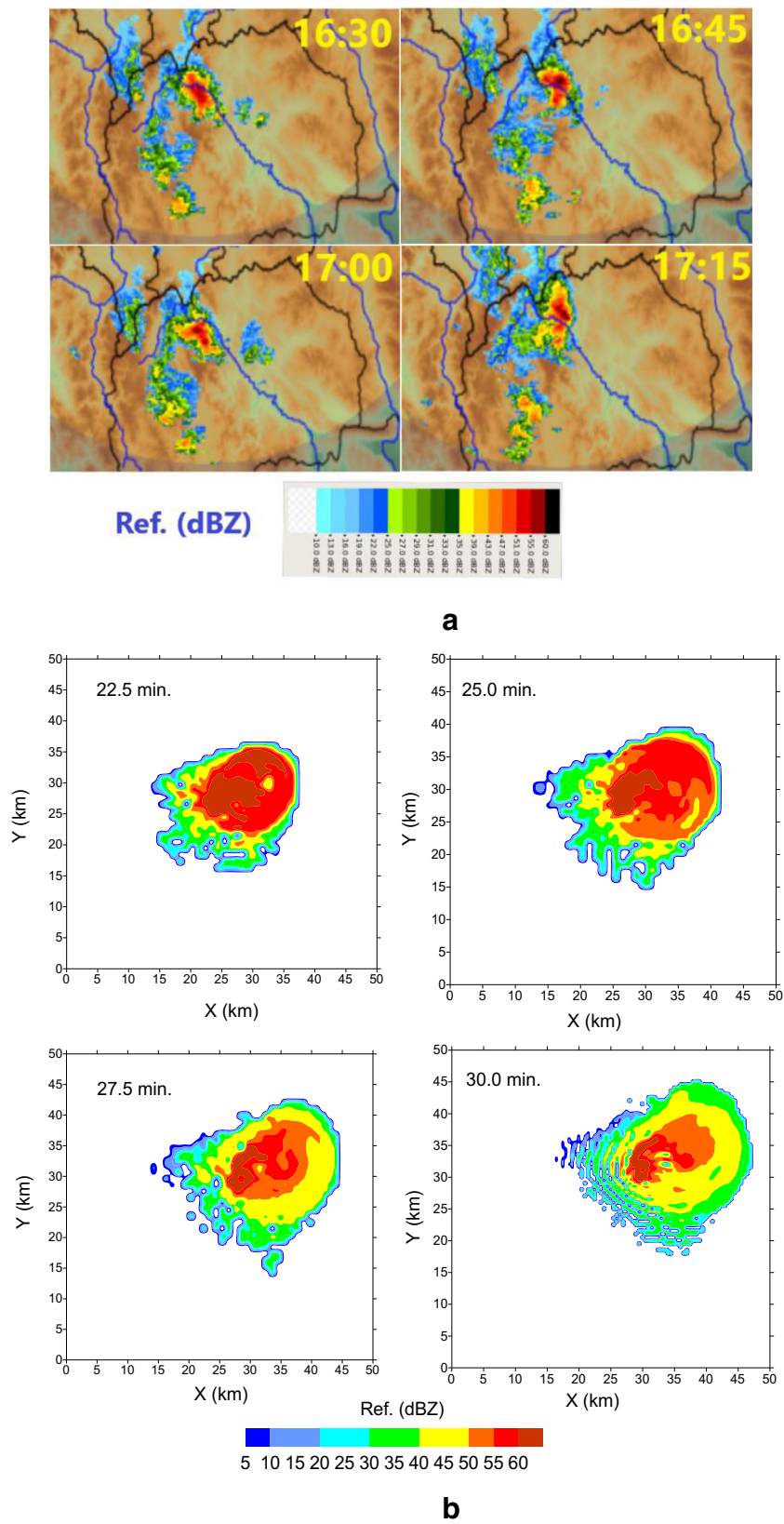


Fig. 13 a) Composite radar reflectivity CAPPI (dBZ) at 2 km height on 6 August 2016 from 17:45–18:30 local time, obtained by RHMS R. Serbia; b) Horizontal transects of the radar reflectivity along SW-NE direction, at the most intense phase of storm evolution

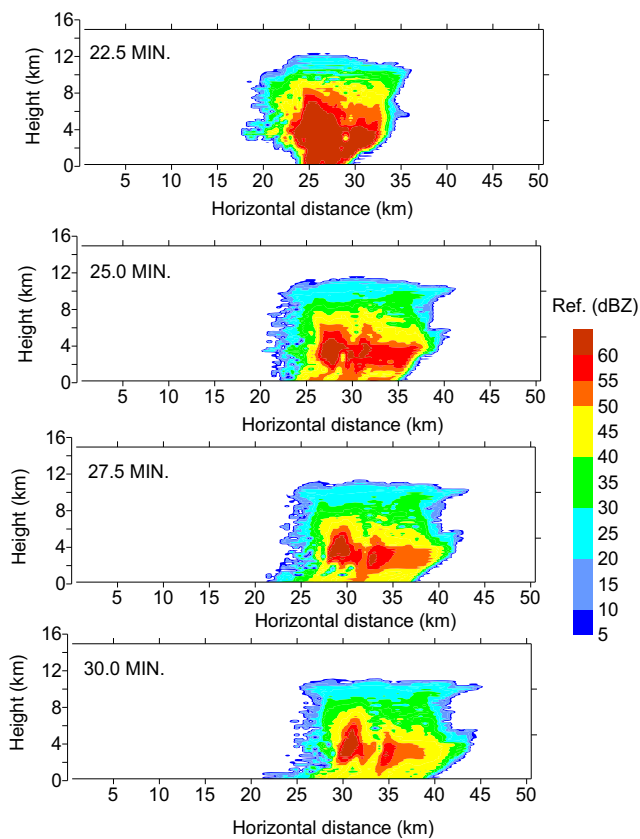


Fig. 14 Vertical (x-z) cross-section of radar reflectivity along SW-NE (upper panel), NW-SE (middle panel), horizontal cross-section at 2 km height in its most intense stage of evolution

The cloud model has demonstrated a good potential in simulation of the supercell convective structure during the most intense stage of evolution from 16:00–17:00 UTC. The horizontal cross-sections of radar reflectivity fields show similar structure relative to the observed reflectivity (Fig. 13) for the same period of time. Especially, the radar echo zone with reflectivity higher than 60 dBZ is well captured by the model. One of the key findings in this research is the radar reflectivity structure and some characteristic signatures which specify the type and the character of the storm. As it is shown on Fig. 14 a high resolution cloud model simulation captured a hook echo, which clearly indicates occurrence of supercell storm with mesocyclone. It well to mentioned that some national weather services may consider the presence of a hook echo as sufficient to justify issuing heavy rainfall and a tornado warning. For comparison we have also shown a conceptual model of a hook echo signature (see Fig. 14). It is evident that the simulated horizontal cross section of the reflectivity at 3.5 km height coincides well with the typical signature illustrated by the conceptual model. In addition to similarities in shape and characteristic structure of radar reflectivity, vertical cross section of radar reflectivity (see Fig. 15) indicates the presence of a bounded weak echo region (BWER) which again imply about the characteristic feature and type of supercell storm. Regarding

the precipitation the numerical simulation indicates that within 60 min simulation time that corresponds with 17:30–18:30 local time, the total accumulated amount of rainfall reaches 131.5 mm (see Fig. 16) which slightly overestimates the total rainfall registered at AMS “Gazi Baba” (source: HMS), of 107 mm for the period of 17:00–22:30. Based on the simulated values it is obvious that the extreme rainfall intensity happened on small limited area of 10–15 km² approximately. The larger domain that was also affected with heavy precipitation core covered 50 km². What is the most characteristic is the extreme rainfall intensity in three successive times, in the limited area with short time duration. The average intensity of falls (10 mm/5 min) during 1 hour simulation time, shows a slightly larger amount relative to the maximum observed rainfall intensity at the Automatic Meteorological Station AMS-“Gazi Baba” at 17:50 local time (source: HMS). Hence, there is the real estimation that during the force of the storm wave in the most affected area, the heavy rainfall intensity is really being extreme. That was also indicated by the results from the simulation. Undeniable is the fact, that such extreme intensity of falls is a rear feature of areas, where there are favorable conditions for the tropical convection, in the presence of extreme heat and moisture in the near surface layer, as it is a case of the tropical cyclones and storms. Table 2 lists the basic parameters of simulated three-dimensional supercell storm on 6 August 2016, which clearly indicates the severity of this type of weather phenomena and could serve as supportive criteria parameters for operational practice of forecasters for early warning of convective weather risks.

4 Discussion with Conclusions

Originally, the scientific examination confirms that severe supercell storm with mesocyclone has been developed with two separate zones with heavy rainfall which falls within 20 min. The total accumulated precipitation for 60 min simulation is about 123 mm, while the averaged 5 min rainfall intensity is 10 mm/5 min.

The accurate quantitative forecast of the relative intensity of convective rainfall associate with such severe storms is a very complex task and still a big challenge of the scientific community in atmospheric modeling. One of the main reasons for the inability to provide reliable estimation in advance and tracking of this category of destructive storms is their initiation into the atmosphere that occurs as a result of certain thermo-dynamic effects and perturbation of temperature and humidity in the planetary boundary layer (PBL) in particular geographical area. For more detailed representation of atmospheric processes in the meso and local scales, non-hydrostatic models have been used with very fine spatial and temporal resolution in a single area or using the technique of nesting. These models have an advantage over those with sparse-resolution, exactly in accurate forecast of such

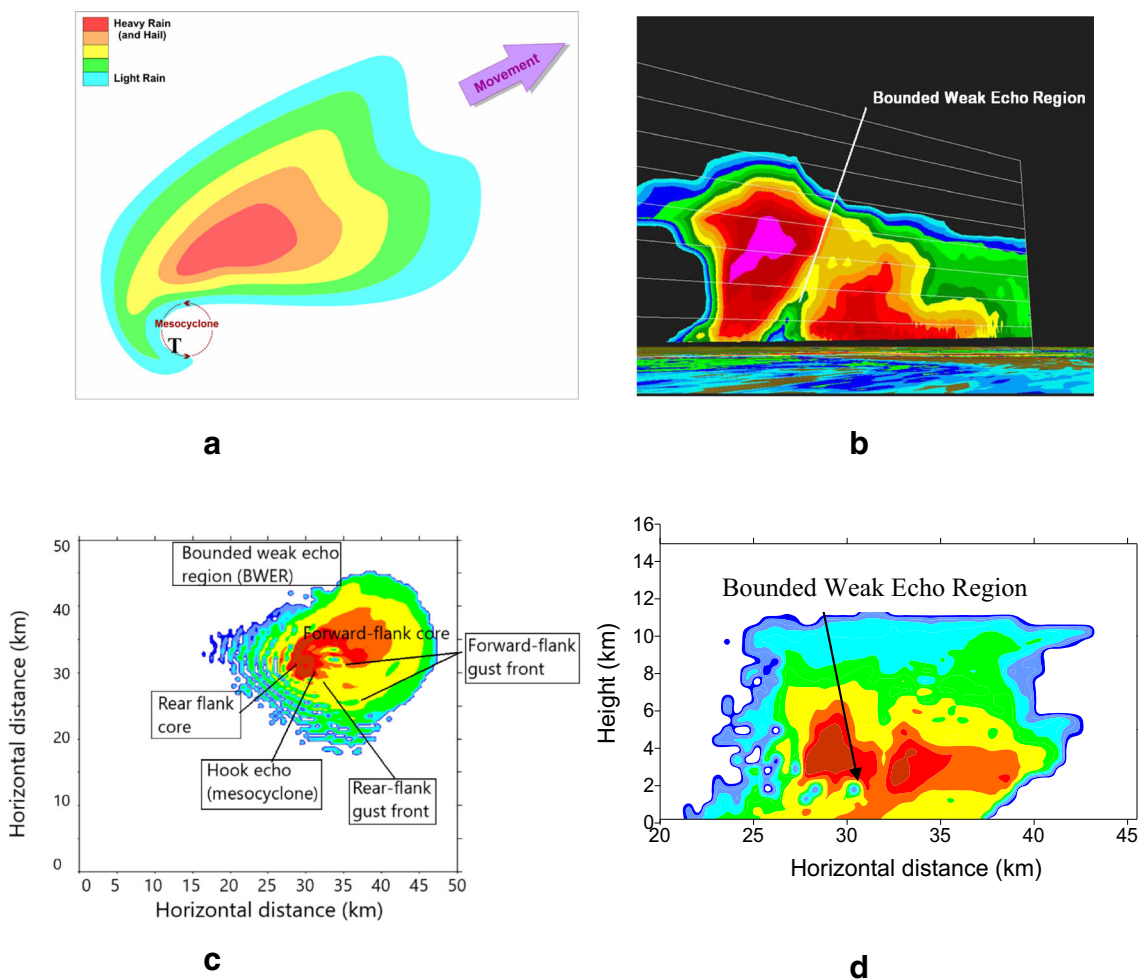


Fig. 15 The conceptual model of supercell storm. (Source: The Pennsylvania State University-Department of Meteorology. **a**) The idealized radar reflectivity of a supercell with the hook echo in concert with the cyclonic circulation associated with the mesocyclone; **b**) A cross section through a supercell. The updraft appears as a minimum in radar

reflectivity called a Bounded Weak Echo Region (BWER); **c**) Modeled hook echo with mesocyclone identified at 3.5 km height in 30 min of the simulation time of supercell storm on 6 August 2016; **d**) Modeled bounded weak echo region identified on a vertical cross section of radar reflectivity

intense convective processes, the structure and evolution of storms systems and distribution of precipitation, but in certain situations they overestimate or underestimate the relative intensity of heavy convective rainfall. These atmospheric processes related to convective storms, which are initiated, evolved and inflamed in a very short period of time on a small-scale are still the main concern of the atmospheric science worldwide. There is no doubt that in the most developed countries, services within their daily operational practice, despite the advanced technology, supercomputing centers, modern technical resources and existence of advanced meteorological alarm systems sometimes face gaps in assessment of the category and the strength of convective storms which initiate and develop at unstable atmospheric conditions with particular extreme weather events with large destructive influences. The nonlinear and wave nature of atmospheric processes has a spatial and temporal variability of processes. Also, the configuration of operating systems for numerical forecast exceeds current limit of computer possibilities, especially for

countries that cover larger geographic areas. In operating practices, in addition to data from numerical models, the NMHS use other products derived from remote measurements (remote sensing control) such as: modern Doppler radar with dual polarization, lidars, sodars, satellites or automatic weather stations, which provide continuous monitoring of the state of the atmosphere, the initiation and development of clouds, their movements, dynamic, microphysical processes and precipitation. Hence, there is a need to develop a comprehensive integrated complex now-casting system for very short-range weather forecast and early warning of natural disasters, as it is envisaged by the World Meteorological Organisation. Basically, scientific analysis points out to the fact, that on August 6 Skopje area was hit by strong supercell storm with mesocyclone. Based on our detail evaluation, the main triggering factors for initiation of very severe convection were: low and moisture inflow, a positive potential vorticity anomaly, low-level directional wind shear, near surface convergence, high helicity index, CAPE and LI. This is one of

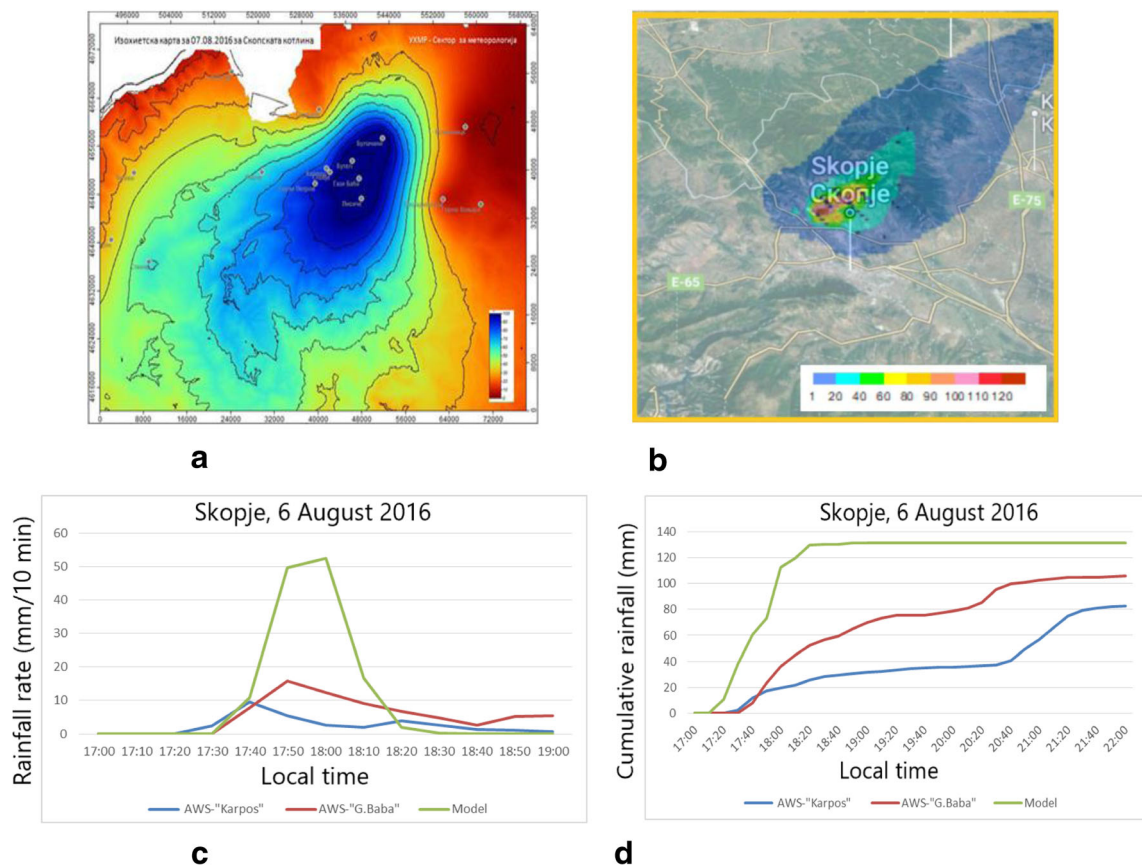


Fig. 16 a) Isohyet chart of the total accumulated rainfall (mm/24 h) in the north-western part of Macedonia observed on 6 August 2016; b) Model simulated total accumulated rainfall and hailfall (kg/m^2) during simulation time; c) The relative intensity of rainfall (mm/10 min) from 1700 to 1900 local time; d) Cumulative observed vs modeled rainfall in mm from 1700 to 2200

Table 2 List of the basic storm ingredients based on cloud model simulation

Parameter	Value
Cloud base	1.6 km
Cloud overshooting top	15 km
Maximum updraft	35 m/s
Maximum downdraft	15.6 m/s
Maximum horizontal wind gust	40 m/s
The rate of change of vertical component of relative vorticity at grid point	-2.942 s^{-2}
Vertical wind shear	$3.8 \times 10^{-3} \text{ s}^{-1}$
Total accumulated rainfall during 1 h simulation time	131.5 mm or kg/m^2
Maximum radar reflectivity which reflects the storm intensity	74.5 dBZ
A hook echo signature	supercell
A bounded weak echo region (BWER)	supercell
Total accumulated rainfall during 2 h simulation time	131.5 mm or kg/m^2
The model averaged rainfall intensity	38 mm/5 min (mean rate of three successive peaks)
Estimated area with extreme rainfall	10–15 km^2
Wider area affected by heavy rainfall	30–50 km^2
Mean storm movement	35 km/h

the most disastrous type of storms with rising rotating air updrafts, intensive initiation and evolution of supercells echoes, production of intense rainfall core, strong and frequent thunder and lightning and longer life cycle of the storm.

The maximum top of the cloud penetrates the troposphere and extends up to 15 km. The maximum vertical speed of 100 km/h and the maximum horizontal speed of about 115 km/h. One of the essential factors according to scientific findings, which were key to the flash flooding, is extreme intensity of rainfall (10 mm/5 min) on average during the simulation of 1 h, fallout in a localized area of 10–15 km². The catastrophic storm that hit Skopje city was unusual for continental areas and more like a tropical storm. Three-dimensional simulation gives a very realistic picture of the nature and severity of this rare destructive weather phenomenon. As summarize-we believe that the scientific overview will at least help in the information on the initiation and evolution of such extreme atmospheric phenomena. We are also confident that this novel scientific method showed a good potential in more realistic simulation of the devastating intensity of this supercell storm with mesocyclone which hit the city of Skopje and the surrounding area and caused people loses and significant material damages.

Acknowledgements Open access funding provided by University of Vienna.

Appendix 1

List of symbols and description of the terms for the cloud physics processes simulated in the model.

Notation	Description.
PIACR	production rate for accretion of rain by cloud ice.
PRAUT	production rate for autoconversion of cloud water to form rain.
PRACW	production rate for accretion of cloud water by rain.
PRACS	production rate for accretion of snow by rain.
PRACI	production rate for accretion of cloud ice by rain.
PREVP	production rate for rain evaporation.
PSACW	production rate for accretion of cloud water by snow.
PSACR	production rate for accretion of rain by snow.
PSAUT	production rate for autoconversion of cloud ice to form snow.
PSACI	production rate for accretion of cloud ice by snow.
PSFW	production rate for Bergeron process-transfer of cloud water to form snow.
PSFI	production rate for Bergeron process embryos (cloud ice) used to calculate transfer rate of cloud ice to snow.
PSMLT	production rate for snow melting to form rain.
PSDEP	production rate for depositional growth of snow.

PSSUB production rate for sublimation of snow.

PGDRY dry growth of graupel; involves PGACS, PGACI, PGACW and PGACR.

PGWET.

wet growth of graupel; may involve PGACS and PGACI and must include PGACW or PGACR, or both (The amount of PGACW which is not able to freeze is shed to rain.)

PGFR probabilistic freezing of rain to form graupel.

PGACW production rate for accretion of cloud water by graupel.

PGMLT production rate for graupel melting to form rain, $T \geq T_0$.

PGACS production rate for accretion of snow by graupel.

PGAUT production rate for autoconversion of snow to form graupel.

PGACR production rate for accretion of rain by graupel.

PGACI production rate for accretion of cloud ice by graupel.

PGSUB production rate for graupel sublimation.

Open Access This article is distributed under the terms of the Creative Commons Attribution 4.0 International License (<http://creativecommons.org/licenses/by/4.0/>), which permits unrestricted use, distribution, and reproduction in any medium, provided you give appropriate credit to the original author(s) and the source, provide a link to the Creative Commons license, and indicate if changes were made.

Publisher's Note Springer Nature remains neutral with regard to jurisdictional claims in published maps and institutional affiliations.

References

- Arakawa, A., Lamb, V.R.: Computational design of the basic dynamical processes of the UCLA general circulation model. In: *Methods of Computational Physics*, vol. 17, pp. 173–265. Academic Press, New York (1977)
- Baldauf, M., Seifert, A., Forstner, J., Majewski, D., Raschendorfer, M.: Operational convective-scale numerical weather prediction with the COSMO model: description and sensitivities. *Mon. Weather Rev.* **139**, 3887–3905 (2011)
- Barth, M.C., Kim, S.-W., Wang, C., Pickering, K.E., Ott, L.E., Stenchikov, G., Leriche, M., Cautenet, S., Pinty, J.-P., Barthe, C., Mari, C., Helsen, J.H., Farley, R.D., Fridlind, A.M., Ackerman, A.S., Spiridonov, V., Telenta, B.: Cloud-scale model intercomparison of chemical constituent transport in deep convection. *Atmos. Chem. Phys.* **7**, 4709–4731 (2007)
- Browning, K.A.: The cellular structure of convective storms, *met. Magazine.* **91**, 341–350 (1962)
- Browning, K.A.: Airflow and precipitation trajectories within severe local storms which travel to the right of the mean wind. *J. Atmos. Sci.* **21**, 634–639 (1964)
- Čurić, M., Janc, D.: Differential heating influence on hailstorm vortex pair evolution. *Q. J. R. Meteorol. Soc.* **138**, 72–80 (2012)
- Čurić, M., Janc, D., Vučković, V.: The influence of merging and individual storm splitting on mesoscale convective system formation. *Atmos. Res.* **93**, 21–29 (2009)



- Doswell, C. A., III, H. E. Brooks, and R. A. Maddox, 1996: Flash flood forecasting: An ingredients-based methodology. *Wea. Forecasting*, **11**, 560–581, [https://doi.org/10.1175/1520-0434\(1996\)011<0560:FFFAIB.2.0.CO;2](https://doi.org/10.1175/1520-0434(1996)011<0560:FFFAIB.2.0.CO;2)
- Hong, S.-Y., Lim, J.-O.J.: The WRF single-moment 6-class microphysics scheme (WSM6). *J. Korean Meteor. Soc.* **42**, 129–151 (2006)
- Hong, S., Noh, Y., Dudhia, J.: A new vertical diffusion package with an explicit treatment of entrainment processes. *Mon. Wea. Rev.* **134**, 2318–2341 (2006). <https://doi.org/10.1175/MWR3199.1>
- Hsie, E.-Y., Farley, R.D., Orville, R.D.: Numerical simulation of ice-phase convective cloud seeding. *J. Appl. Meteorol.* **19**, 950–977 (1980)
- Jacques, D., Chang, W., Baek, S.-J., Fillion, L.: Developing a convective-scale EnKF data assimilation system for the Canadian MEOPAR project. *Mon. Wea. Rev.* **145**, 1473–1494 (2017). <https://doi.org/10.1175/MWR-D-16-0135.1>
- Janjic, Z.I.: A nonhydrostatic model based on a new approach. *Meteorog. Atmos. Phys.* **82**, 271–285 (2003)
- Klemp, J.B.: Advances in the WRF-NMM model for convection-resolving forecasting. *Adv. Geosci.* **7**, 25–29 (2006)
- Klemp, J.B., Wilhelmson, R.B.: The simulation of three-dimensional convective storm dynamics. *J. Atmos. Sci.* **35**, 1070–1096 (1978)
- Lin, Y.L., Farley, R.D., Orville, H.D.: Bulk water parameterization in a cloud model. *J. Climate Appl. Meteorologie.* **22**, 1065–1092 (1983)
- Litta, A.J., Mohanty, U.C.: Simulation of severe thunderstorm event during the field experiment of STORM programme 2006, using WRF-NMM model. *Curr. Sci.* **95**(2), 204–215 (2008)
- Litta, A.J., S. M. Ididcula, U. C. Mohanty, and S. K. Prasad, 2011: Comparison of thunderstorm Simulations from WRF-NMM-NMM and WRF-NMM-ARW models over east Indian region. *The scientific world journal* volume 2012, article ID 951870, 20 pages <https://doi.org/10.1100/2012/951870>
- Lompar, M., Ćurić, M., Romanic, D.: Simulation of a severe convective storm using a numerical model with explicitly incorporated aerosols. *Atmos. Res.* **194**, 164–177 (2017)
- Orville, H.D., Kopp, F.J.: Numerical simulation of the history of a hail-storm. *J. Atmos. Sci.* **34**, 1596–1618 (1977)
- Poterjoy, J., Anderson, J., Sobash, R.: Convective-scale data assimilation for the weather research and forecasting model using the local particle filter. *Mon. Weather Rev.* **145**, 1897–1918 (2017) [1175/MWR-D-16-0298.1](https://doi.org/10.1175/MWR-D-16-0298.1)
- Potvin, C.K., Flora, M.L.: Sensitivity of idealized supercell simulation to horizontal grid spacing: implications for warn-on-forecast. *Mon. Weather Rev.* **143**, 2998–3024 (2015). <https://doi.org/10.1175/MWR-D-14-00416.1>
- Spiridonov, V., Ćurić, M.: The relative importance of scavenging, oxidation, and ice-phase processes in the production and wet deposition of sulfate. *J. Atmos. Sci.* **62**, 2118–2135 (2005)
- Spiridonov, V., Curic, M.: A storm modeling system as an advanced tool in prediction of well organized slowly moving convective cloud system and early warning of severe weather risk. *Asia-Pac. J. Atmos. Sci.* **51**(1), 1–15 (2015). <https://doi.org/10.1007/s13143-000-0000-0>
- Spiridonov, V., Dimitrovski, Z., Ćurić, M.: A three-dimensional simulation of supercell convective storm. *Adv. Meteorol.* **2010**, 15 (2010)
- Sun, J., Chen, M., Wang, Y.: A frequent-updating analysis system based on radar, surface, and mesoscale model data for the Beijing 2008 forecast demonstration project. *Weather Forecast.* **25**, 1715–1735 (2010)
- Telenta, B., Aleksic, N.: A three-dimensional simulation of the 17 June 1978 HIPLEX case with observed ice multiplication, 2nd international cloud modeling workshop, Toulouse, 8-12 august 1988. *WMO/TD No.* **268**, 277–285 (1988)
- Warner, T.T.: *Numerical Weather and Climate Prediction*, p. 526. Cambridge University Press, Cambridge (2011)